Applications

After a treatment of the basic phenomena and some examples, here there will be discussed some applications, taking the former as known.

Interference by division of amplitude:
Fabry-Perot Interferometer

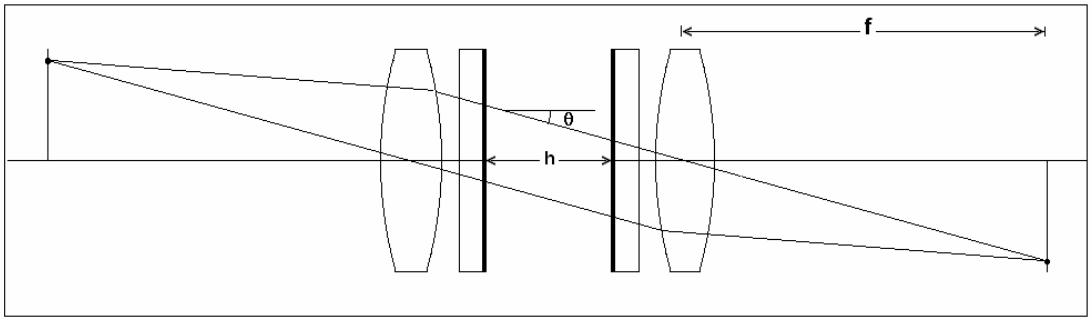

Fig. 5.1

Multiple beam theory permits to make a model of the Fabry - Perot interferometer, Fig 5.1

The first lens has its focus in the extended image given by the telescope, and the second lens in the detector.

Between both, there is a space of collimated light where is the interferometer, composed of two partially transparent parallel flat mirrors, separated by a distance *h*. Each point of the image subtends an angle θ in the space of collimated light. If it is monochromatic, there are formed fringes of equal inclination, that in the focus of the second lens are fine concentric circles, Fig. 5.2 (a),(b),(c)

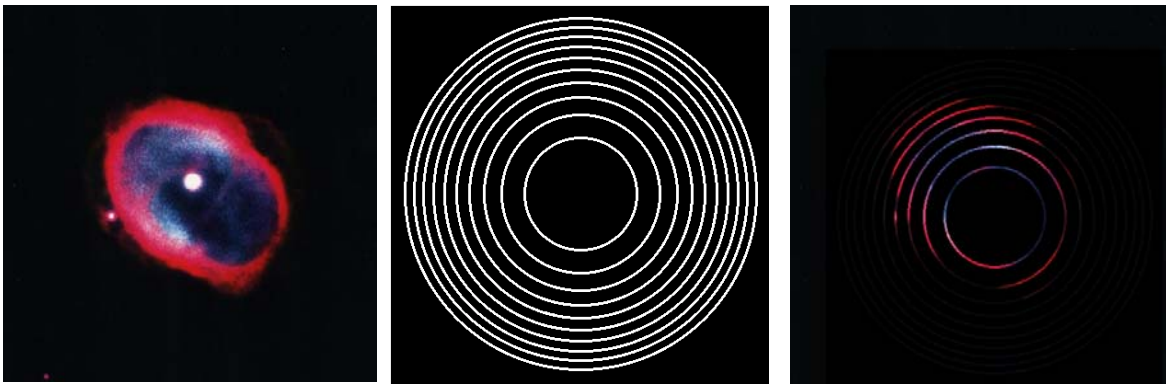

Fig 5.2 (a) (b) (c)

(a) is a photograph of a planetary nebula, extended object with a line spectrum, quite adequate for this case. (b) are artificial synthetic fringes, and (c) is a superposition of both, as they would appear in the focus of the second lens. All this is schematic due to lack of an actual photograph, and for instance, a well noticeable error is that the fringes should break on passing from red to blue.

The light pattern in the image is modulated by the circles. The intensity profile in each circular fringe is given by equation (2.23) complemented with (2.9). This is the instrumental function.

In equation (2.9), the only factor that changes δ is θ_2 (From now on θ, and besides, $n_2 = n$)

Let's assume that for $\theta = 0$ the order of interference is *m,* that is $\delta = 2m\pi$. As the optical thickness *decreases* with inclination, there is an angle for which the order of interference is $2(m-k)\pi$, where *k* is the number of the *k- th* circle.

Then

(5.1) $$\frac{2nh}{\lambda} = m \quad \text{and} \quad \frac{2nh\cos\theta}{\lambda} = m - k$$

(5.2) $$\frac{2nh(1-\cos\theta)}{\lambda} = k \approx \frac{nh\theta^2}{\lambda}$$

The *k-th* circle has radius

(5.3) $$r = f\theta = f\sqrt{\frac{k\lambda}{nh}}$$

The circles has radii proportional to $\sqrt{k}$, as in the well known Newton rings. But there is an important difference: these are of equal inclination, and Newton's are of equal thickness.

If the plates move away, the circles gets bigger and disappear at the border, while others appear at the center.

Let us see what happens at the center of the plate if the interference order increases by one.

Free spectral range

(5.4) $$\lambda_1 = \left(\frac{2nh}{m}\right) \quad , \quad \lambda_2 = \left(\frac{2nh}{m+1}\right) < \lambda_1$$

(5.5) $$\lambda_1 - \lambda_2 = \frac{2nh}{m(m+1)}$$

This wavelength difference is the free spectral range, analogous to that was defined for the diffraction grating.

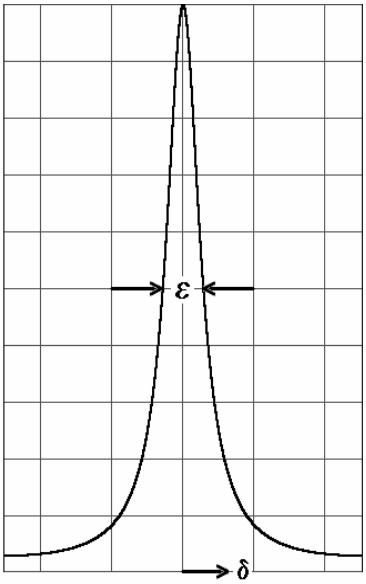

Fig 5.3

Resolving power

To find the resolving power, it is needed to know the width of the fringe.

The interval of δ between fringes is 2π . In order to find the width ε at half height we see from Fig. 5.3 and from equation (2.26), that the border is defined by

(5.4) $$\frac{1}{2} = \frac{1}{1 + F\sin^2\frac{\varepsilon}{4}}$$

If the fringe is fine, is

(5.5) $$\sin^2\frac{\varepsilon}{4} \approx \frac{\varepsilon^2}{16}$$

(5.6) $$1 + \frac{F\varepsilon^2}{16} = 2$$

(5.7) $$|\varepsilon| = \frac{4}{\sqrt{F}} = \frac{4\pi nh\delta\lambda}{\lambda^2}$$

A parameter "finesse" F is defined as the ratio of the interval between fringes and its width.

(5.8) $$\mathrm{F} = \frac{2\pi}{\varepsilon} = \frac{\pi\sqrt{F}}{2}$$

As $nh = \frac{m\lambda}{2}$, results

(5.9) $$\frac{\lambda}{\delta\lambda} = \frac{m\pi\sqrt{F}}{2} = m\,\mathrm{F}$$

Comparison with a diffraction grating.

In the grating there is a finite sum of equal amplitudes, and here the sum extends to an infinite number of decreasing amplitudes. Hence it may be considered F as an effective number of beams that represents approximately the instrumental function, so there is analogy between equations (5.9) and (3.50). The finite number of beams in the grating produces the secondary lobes in (3.46), that are absent in (2.26). This phenomenon is what is called "ringing" in the theory of Fourier series. Both configurations almost merge in the echelon.

Construction details

In order to scan the instrumental function along a free spectral range, it may be varied *n* or *h*. The motion of the plates, if *h* is varied, needs to be so precise that it must be resorted to piezoelectric systems, in which a crystal is strained by an electric field. To vary *n,* there may be changed the air pressure in the space between plates.

As the resolving power increases with reflectivity, it is necessary to use mirrors of low absorption and a thickness such that the transmitted fraction be small (see formula (2.27)). The best metal is silver, but it soon tarnishes in the air. The best technical solution is to put dielectric mirrors of type $n_0[HL]^N n_s$, that should have zero absorption because their indices are in principle real.

In practice there is a small absorption depending on the conditions of fabrication.

The tolerance in surface flatness is more stringent with decreasing fringe width, because it must be a fraction of $\delta\lambda$.

Therefore a Fabry-Perot interferometer is a delicate piece of high precision.

Is amazing how all light pass through two successive mirrors when hardly it can pass trough just one. If the reflectivity is, for instance, 0.95 and there is no absorption, the transmissivity of the whole is $(1-0.95)^2 = 0.0025$. Nevertheless, all light pass trough. This is because the separation between mirrors is $m\lambda/2$, and the several waves reaching the mirrors with path difference $m\lambda$ are reinforced. If the reflectivity is very high, there are more waves summed and the result is the same, but the interval of λ in which they are reinforced is narrower.

The F-P is a "resonant cavity", and works like a radio tuner. It is possible to trace the evolution of tuners from coil and condenser to the F-P according the wavelength shortens.

If an "active" medium is placed in the spacer (definition to look for in books on quantum optics), a laser is obtained.

Dielectric mirror

A dielectric mirror has a maximum reflectivity given by equation (2.64) for the wavelength in which all layers has $\lambda/4$ optical thickness.

In order to find what happens in a whole spectral range, a numerical application of the Abeles – Herpin method must be made.

The result is shown in Fig. 5.4 for a multilayer of 17 layers whose prescription is $1.52L\,[HL]^8 1$, with $n_H = 2.3$, $n_L = 1.38$.

The layer thickness are $h_L = 1085\ A$, $h_H = 651\ A$, and the reflectivity has a maximum $R = 0.9986$ for $\lambda = 5990\ A$.

It is seen a wide band of high reflectivity flanked by zones of oscillation.

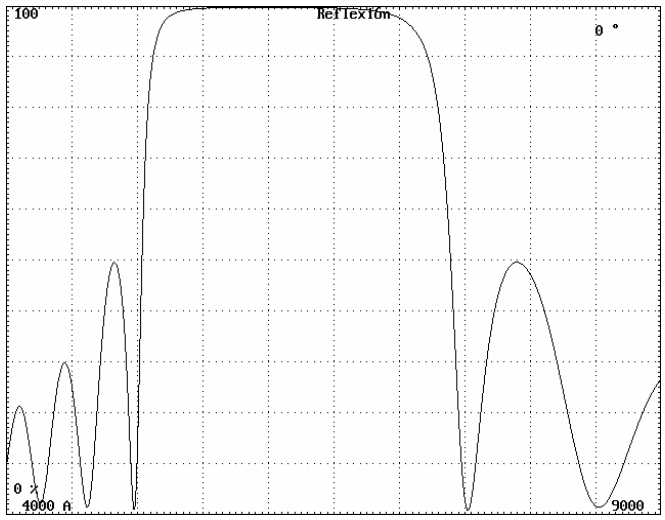

Fig. 5.4

Band – pass filter

If the central thickness (number 9) is doubled, there appears two dielectric mirrors of 8 layers separated by a $\lambda/2$ spacer, that is, an extra-flat Fabry-Perot of order *1.* The transmission characteristic of that multilayer *(1-R,* for there is no absorption) is shown in Fig. 5.5. We have obtained a narrow pass filter, and besides, we proved that the Fabry-Perot can be modelled with matrices with more detail than summing multiple beams.

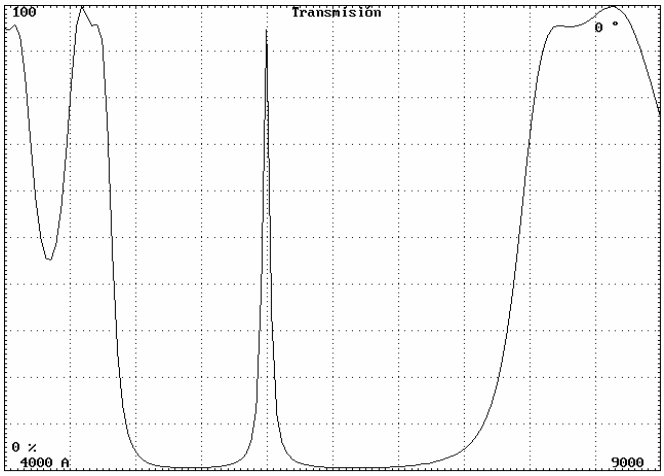

Fig. 5.5

Equation (2.9) allows a prediction of the general behavior of the filter, and of any multilayer, with increasing incidence angle: as the optical thickness decreases the interference condition occurring for a given λ will occur for a shorter λ.

As an example, if the interference condition consists of a transmission band, that band shifts to violet with a tilt of the filter.

Within certain limits, the filter may be tuned with this effect. It is often used for measuring radial velocities in extended starfields.

The band shift has a bad consequence in a strongly convergent beam, because light coming from the rim of the cone is shifted to violet, while that coming from the center is not, and the band is asymmetrically widened (only shifts the violet flank). The tilt also produces a splitting of the band in its TE and TM polarization components, but is less noticeable.

Step filter.

The oscillations in one flank of the transmission band can be suppressed by a departure of the condition that all optical thickness to be $\lambda/4$. In this way, one obtains a step filter, useful to separate overlapping orders in a spectrum.

In Fig. 5.6 is shown the spectral response of a step filter optimized from prescription of Fig. 5.4, and in Tab. 5.1 there is the prescription of the aperiodic multilayer.

The index *1.38* is for Magnesium Fluoride, MgF_2; and *2.3* for Zinc Sulphide, *ZnS*. The indices of the initial and final media are *1.52*, common glass *BK7* and *1*, air.The thickness are in *A*

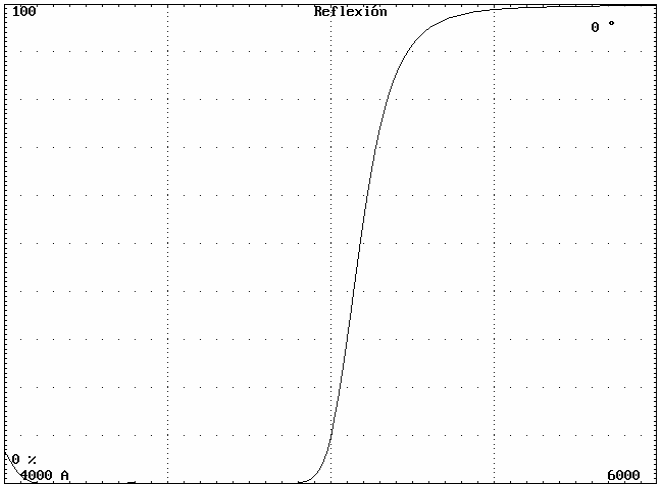

Fig. 5.6

#	*I*	1	2	3	4	5	6	7	8	9	10	11	12	13	14	15	16	17	*F*
n	1.52	1.38	2.3	1.38	2.3	1.38	2.3	1.38	2.3	1.38	2.3	1.38	2.3	1.38	2.3	1.38	2.3	1.38	1
h	–	1227	830	1073	644	1189	630	1066	621	1158	632	1073	633	1175	689	1172	972	984	–

Tab. 5.1

See in annex "Program FILMS". how to design this multilayer

Anti - reflection coatings.

With some willingness we may also call filters to antireflection coatings.

We have seen how to design a simple single layer and how to take the problem of one with several layers by the method of closing the polygonal.

In Fig 5.7 there are shown the spectral response of a single layer of MgF_2 (a), designed for $\lambda_{min} = 5000\ A$, and a triple one (b), whose prescription is in Tab. 5.2 . The maximum ordinate of the graph is *4%,* near the reflectivity of the glass alone.

The indices 1.38, 2.1 and 1.65 belongs respectively to MgF_2, Zirconium dioxide ZrO_2 and Cerium fluoride CeF_3

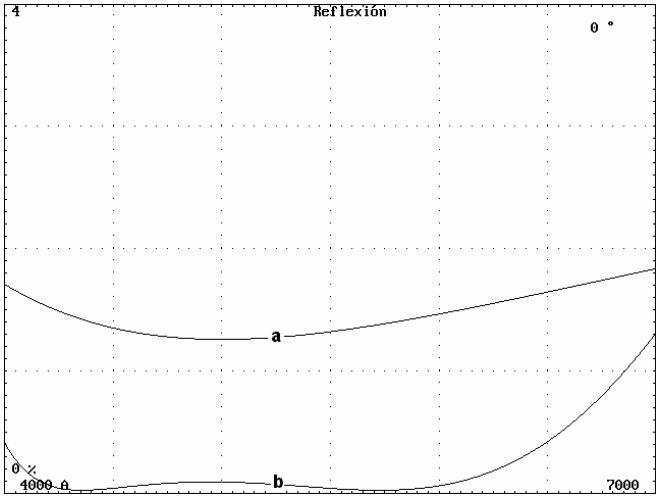

Fig. 5.7

#	*I*	1	2	3	*F*
n	1	1.38	2.1	1.65	1.52
h	–	897	1179	751	–

Tab 5.2

The effect of an antireflection coating may be very important for two reasons: It increases transmitted light and also the contrast, due to suppression of parasitic light reaching the detector via spurious reflections in optical surfaces.

The light transmitted by a system compounded by *N* lens surfaces where each one has reflectivity *R* is approximately $(1-R)^N$. It is taken the intensity and not the amplitude because it is assumed polychromatic light, in a visible band. Let´s assume the lenses having an index *n = 1.52*.

In Tab 5.3 there is the fractional transmitted light as a function of *N* with antireflectants (b),(a) and nothing. One can check the viability of optical systems with many surfaces.

Tab. 5.3

N	*2*	*4*	*8*	*16*	*32*	*64*
b	*0.9981*	*0.9962*	*0.9925*	*0.9851*	*0.9703*	*0.9416*
a	*0.9749*	*0.9505*	*0.9035*	*0.8164*	*0.6665*	*0.4441*
–	*0.9178*	*0.8423*	*0.7094*	*0.5033*	*0.2533*	*0.0642*

Interference by division of wavefront

Diffraction grating spectroscopes

It has been studied in some detail the workings of the grating, the most common device in spectroscopy. Now we will see which elements form the optical train to produce a spectrum, and for clarity they will be shown first in a simplified scheme where still is not included the grating,

A slit of width *a* is placed at the image given by the telescope. On the slit is the focus of a collimator that from each point of the slit produces parallel beams in a space where will go the grating.

The beams are collected by a camera, and in its focus there is formed an image of the slit, of width *a'*. Here, as in the Fabry-Perot, the dispersing element is placed in a space of collimated light.

. From the figure it is seen that to avoid light loss it must be

(5.10) $$\frac{f_{te}}{D_{te}} = \frac{f_{co}}{D_{co}}$$

The angle subtended by *a* on the collimator is a / f_{co}. The parallel emerging beams incide on the camera *with the same angle,* then

(5.11) $$a' = a\,\frac{f_{ca}}{f_{co}}$$

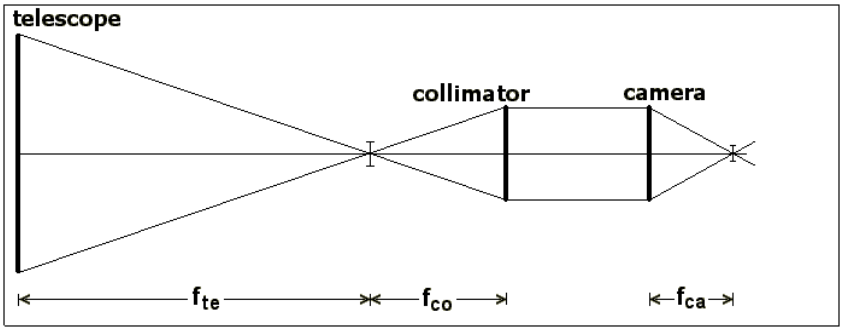

Fig. 5.8

Before the grating is introduced, let us discuss a practical issue.

At the focus of the telescope, an image is formed with extension *s* due to seeing. To avoid light loss, the slit must have a width $a = s$, unless it is used a device to redirect the light falling outside the borders.

The angle subtended by the slit over the sky in these conditions is

(5.12) $$\alpha_s = \frac{a}{f_{te}}$$

Typically, α_s is roughly *1"*, although depending on the place and atmospheric conditions it may lie between *0.5"* and *2"*.

It is also desirable for a' to be of the same magnitude as the resolution element of the detector, for instance, in a CCD, 2 pixels. Let us call this Δ.

In the simple scheme one may assume that $D_{ca} = D_{co} = D$.

Hence

(5.13) $$\Delta = \frac{a\, f_{ca}}{f_{co}} = \frac{\alpha_s\, f_{te}\, f_{ca}}{f_{co}} = \frac{\alpha_s\, f_{ca}\, D_{te}}{D}$$

That is

(5.14) $$\frac{f_{ca}}{D} = \frac{\Delta}{\alpha_s\, D_{te}}$$

This means that the larger the telescope or the worst the seeing, the greater the relative aperture of the camera, and the most difficult its design.

These factors influence the geometrical size of the slit image.

Now enters the grating, supposed plane.

The reason to place it in a space of collimated light is that all rays incide with the same angle.

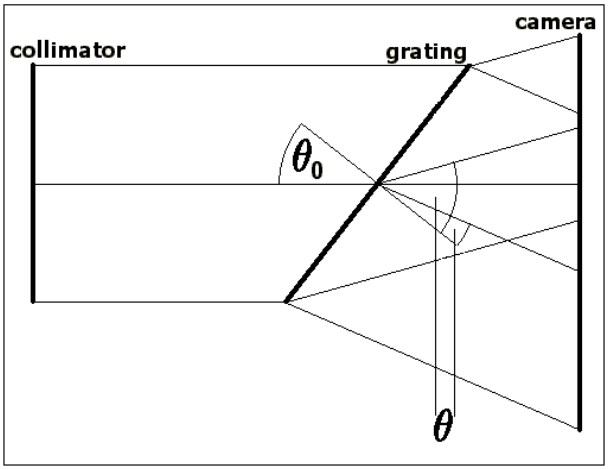

Fig. 5.9

The dispersion has several consequences

1) – From the grating there issues a fan of collimated monochromatic beams, that is, the grating is the pupil of the camera.

Hence, the camera must have a larger relative aperture to accept all them. To fulfill the demand of large relative aperture, it is often used a Schmidt camera but the above prevents the normal configuration, with the entrance pupil on the correcting plate. A Bowers corrector may be better.

2) – The ratio $a' = a\, f_{ca} / f_{co}$ is no longer valid in the direction of dispersion, because the exit angle from the grating is not the same a / f_{co} as at the entrance.

To see why is it, we use the grating equation (3.47)

$$\sin\theta = \sin\ \theta_0 + \frac{m\,\lambda}{d}$$

If θ_0 change by the small angle $a / f_{co} = \delta\theta_0$, it is

(5.15) $$\delta\theta = \frac{\cos\theta_0}{\cos\theta}\ \delta\theta_0$$

The ratio $\cos\theta_0 / \cos\theta$ is called "amorphic factor", and it may be easily seen that it is the ratio D_0 / D between the incident and diffracted beams. The amorphic factor vary with the diffraction angle, and so the width of the slit image. The name comes from the fact that the magnification is different in the direction of dispersion than in a normal to it, and the images deform, as in the paintings of El Greco.

Equation (5.11) is modified

(5.16) $$a' = a\,\frac{f_{ca}\cos\theta_0}{f_{co}\ \cos\theta}$$

Resolving power

It was seen before the resolving power of the grating alone, but that of the complete instrument may be different. In what follows we ignore the diffraction effects in lenses and slits.

On the final image, two λ differing by $\delta\lambda$, are separated by a distance

(5.17) $$\delta l = f_{ca}\delta\theta = f_{ca}\left(\frac{d\theta}{d\lambda}\right)\delta\lambda$$

The factor $d\theta / d\lambda$ is the dispersive power, and for a grating it amounts to

(5.18) $$\frac{d\theta}{d\lambda} = \frac{m}{d\ \cos\theta}$$

If both λ are on the verge of being resolved, the rectangular images of the slit are border-to-border and is $\delta l = a'$.

Results

(5.19) $$\delta\lambda = \frac{a'\ d\ \cos\theta}{m\ f_{ca}} = \frac{a\ d\ \cos\theta_0}{m\ f_{co}}$$

Diffraction limit.

In geometrical optics the images of the slit are rectangles, but really their borders are affected by Fraunhofer diffraction fringes produced by the rim of the camera lens. In detail, the profile results from superposition of figures like 3.6 for each point of the slit. The diffraction is also revealed in the collimator: if the slit is closed enough, the diffracted light extends to the border of the collimator lens, and if it is closed still more there is a waste of light without a noticeable change in the width of the image (we assume the diameters of collimator and camera to be similar). By all this, we agree in calling diffraction limit to a slit width so that $\sin\alpha = \lambda / a$, where α is the angle subtended by the radius of the collimator and λ a typical value of the spectrum. That is, the first zero of diffraction by the slit falls in the border of the collimator.

Taking $\sin\alpha \approx D_{co} / 2\ f_{co}$, results

(5.20) $$a = \frac{2\,\lambda f_{co}}{D_{co}}$$

And from all the former, too

(5.21) $$a' = \frac{2\lambda f_{ca}\cos\theta_0}{D_{co}\cos\theta}$$

(5.22) $$\delta l = \frac{m f_{ca}\,\delta\lambda}{d\cos\theta}$$

Taking $a' = \delta l$

(5.23) $$\delta\lambda = \frac{2\lambda d\cos\theta_0}{m D_{co}}$$

The ruled extension of the grating is $L = D_{co} / \cos\theta_0$, and in L enter $N = L / d$ grooves, if the collimator has a large enough diameter.

That is,

(5.24) $$\frac{d\ \cos\theta_0}{D_{co}} = \frac{1}{N}$$

Hence

(5.25) $$\delta\lambda = \frac{2\lambda}{mN}$$

This quantity is of the same magnitude of (3.50). The discrepancy of the factor 2 is due to that the geometrical images are resolved when their separation is *a'* and the corresponding of diffraction when the peak of one fall in the first zero of the other, that is half the former. See also the example in Fig. 3.10 and its comments.

To sum up, if all the elements are correctly dimensioned, *if there are no geometrical aberrations* and if the slit is closed to the value (5.20), the resolving power of the spectroscope is that of its diffraction grating. In any other case is less.

*The resolving power of the spectroscope is independent from the angular resolving power of the telescope. Closing the slit adequately, a good spectroscope with a bad telescope or bad seeing has the same resolution and the only difference is that it does not detect dim objects***.**

In space there is no seeing, and all simplifies.

The diameter of the diffraction image of a star given by the telescope is

(5.26) $$2\rho = \frac{2.44\,\lambda\, f_{te}}{D_{te}}$$

The aperture for maximum resolution is

(5.27) $$a = \frac{2\lambda\, f_{co}}{D_{co}}$$

As the ratios f / D are the same, one gets automatically the maximum spectral and angular resolution, if all is well made. The factor *1.22* is due to the mixing of circular and rectangular apertures, but does not matter very much.

Besides, as the equivalent α_s in formula (5.12) is that of diffraction, the relative aperture of the camera is the least possible.

Geometrical optics.

Design of a refracting telescope objective.

We shall see the performance of a f / 9 – 137 mm diameter refracting objective made with two pairs of glasses

(a)	Crown BK7	Flint F2	(Schott)
(b)	Crown B19-61	Flint C55-40	(Corning France)

Case(a) is with common optical glasses and (b) with an apochromatic combination.

With formulas (4.48) and (4.49) may be estimated the secondary spectrum of both lenses.

Glass	n_F	n_D	n_C	v_D	P_{FD}	
BK7	*1.52238*	*1.51673*	*1.51432*	*64.11*	*0.70100*	$\left\lvert\frac{\Delta f}{f}\right\rvert_{sec} = \frac{1}{1966}$
F2	*1.63209*	*1.61989*	*1.61503*	*36.33*	*0.71513*	
B19-61	*1.52499*	*1.51899*	*1.51653*	*61.35*	*0.70922*	$\left\lvert\frac{\Delta f}{f}\right\rvert_{sec} = \frac{1}{24448}$
C55-40	*1.66697*	*1.65536*	*1.65062*	*40.08*	*0.71009*	

Both lenses are corrected for spherical aberration and coma by an algebraic method which determines the radii of curvature, and generally gives different internal radii, so they cannot be cemented. (Program "G – SUM")

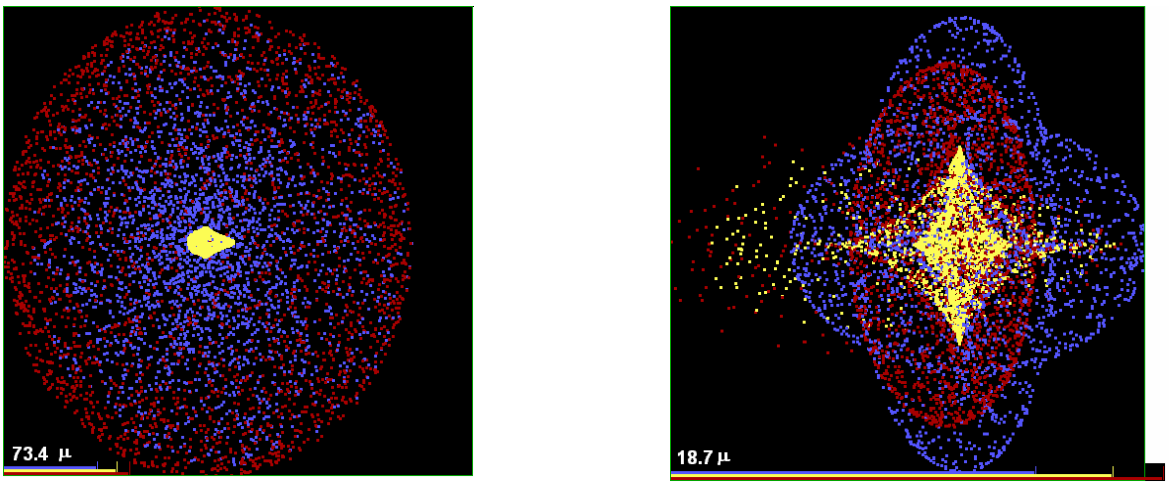

Fig. 5.10 (a) (b)

The exact coincidence of the focal distances was achieved by means of scale factors. The lens prescriptions were retouched with ray tracing to improve the coincidence of the back focal

distances f_p in the extreme colors *F* and *C*, and in case (b) it was introduced a slight asphericity in the last surface because the image is dominated by geometrical aberrations.

They are

i	Radius curv.	Clear radius	Distance	Glass	Comment
	Lens (a)				
1	*751*	*68.5*	*13*	*BK7*	*d*
2	*–451*	*68.5*	*0*	*1*	
3	*–456*	*68.5*	*7*	*F2*	
4	*–1871*	*68.5*	*-*	*1*	
	Lens (b)				
1	*777*	*68.5*	*15*	*B19-61*	*d*
2	*–319*	*68.5*	*0*	*1*	
3	*–331.5*	*68.5*	*7*	*C55-40*	
4	*–1343*	*68.5*	*-*	*1*	*a*

Aspherics

i	Citric const	Asf(4)	Asf(6)	Asf(8)
4	*0.15*	*0*	*0*	*0*

In the last column, "d" means that the surface is considered diaphragm and "a" that is aspheric, what opens a new list of data. The equation of the aspheric surface and the definition of the coefficients are given in equation (4.57).

The central thickness of the glasses are unimportant parameters in this case and they are set for the lens to be thin but robust.The air space in row 2 is zero, but as the lenses has different radii, there is a thin air wedge between both. This parameter is very critical indeed, and the image quality degrades if it is changed. In both cases the lenses touch at the center, as can be seen from the values of the curvature radius 2 and 3. The indicated clear radius permits to mount a *140 mm* diameter lens

The back focal distance f_p of both lenses is *1233 mm*

Fig. 5.10 (a) and (b) are the images produced from an object point at infinity, subtending a semifield angle of $0.5°$.

The images are obtained at the focus of the central color.

The magnitude of the secondary spectrum obtained by ray tracing is very similar to the calculated one if the lenses are kept thin.

There is indicated the extension of the image in microns.

The lower segments are the diameters of the Airy disks in the 3λ. As they are in (b) about the same size as the image, it is concluded that the image is diffraction limited, that is, actually this figure is not seen but a somewhat distorted Airy disk.

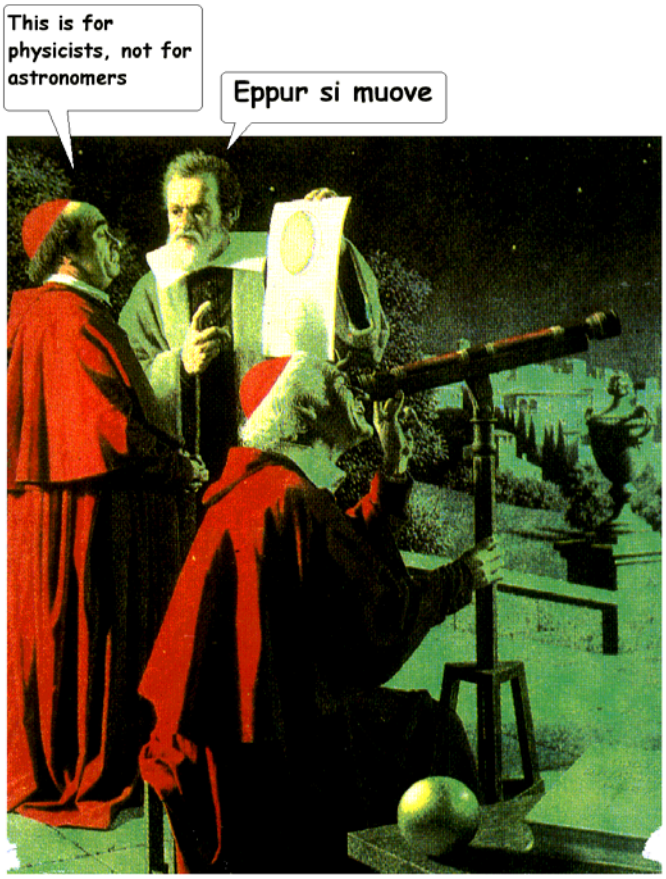

From “Cosmos”, by Carl Sagan

In (a) the image in central λ is similar to (b) in shape an dimensions, but there are two large overlapping halos, red and blue, indicating that these two λ coincide at another focus.

We may call apochromatic that
lens whose chromatic aberrations are about or less than the already small geometrical aberrations.

In practice, the construction of an apochromatic demands great precision in the measurement of the indices. There cannot be used the nominal values of the catalogs and it is necessary a measurement on the actual glass. The departures of the indices from a piece to another does affect the performance. Of course, this implies the need of great precision in the curvatures, centering, etc.

Schmidt camera, theory and design

We have seen that all aberrations except spherical increases with the field angle, that is the distance from the image point to axis. A very elegant way to correct an optical system would be then to invent one with no axis. Let us, for example, imagine a glass sphere. The paraxial focal distance is $f = \frac{n\,R}{2\,(n-1)}$ for light coming from any direction.

But the spherical and chromatic aberration is so large that the system is used only in "heliofanographs", devices in which the image of the Sun burns a sheet of paper as it travels across the sky and record the degree of cloudiness along the day.

The following option is a spherical mirror with its center of curvature on the diaphragm.

The mirror has no chromatic aberration and the spherical is small compared with the former example. But in this case the image interposes in the beam, and it must be accepted a central obstruction. If the diaphragm is small enough respect to the radius of curvature, the spherical aberration will be tolerable. If we want more luminosity, the mirror must be parabolized, and then it has an axis.

Bernhard Schmidt had the idea of dividing tasks; let the mirror to provide luminosity and convergence, and to correct its spherical aberration with a plate in the right place, that is, in the diaphragm.The plate introduces a spherical aberration of opposite sign, and on arriving the light to the mirror it cancels out. The plate is more complex than a lens, and it has an axis, but its profile is very shallow, indistinguishable at first sight from a plane parallel plate, so that the higher order aberrations introduced are very small.

Is important to note that the basic concept of Schmidt is not the correcting plate, but the location of the diaphragm.

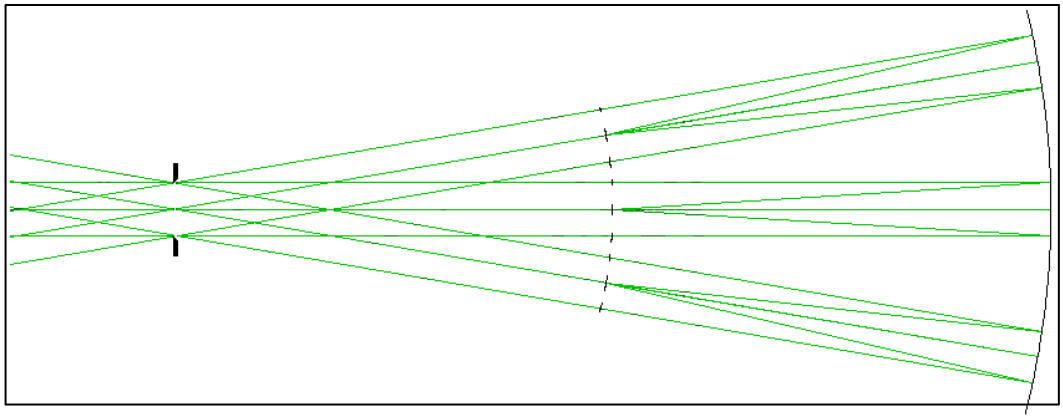

Fig. 5.11

To illustrate the point, let us suppose a spherical mirror with aperture small enough as to its spherical aberration be tolerable, for example, an *f / 8* , *10 cm* diameter mirror, Fig. 5.11. It is not needed a correcting plate, but the oblique beams introduce the other aberrations

Placing a diaphragm at the radius of curvature, each oblique beam continues falling normally on a different portion of the mirror. For this reason there are no oblique aberrations, except field curvature, that results from the very symmetry.

Derivation of the plate profile

In Fig. 5.12 there is a spherical mirror, and a ray passing through Q parallel to an axis at height y intersects it at M

In what follows, often the = sign really means $\approx$ but the reader will know how to tell them apart by making the calculations.

$$\overline{OM} = \overline{QM} = \frac{R}{2\cos\theta} = \frac{R}{2\sqrt{1-\sin^2\theta}} = \frac{R}{2\sqrt{1-\frac{y^2}{R^2}}}$$

(5.28)
$$= \frac{R}{2\left(1-\frac{y^2}{2R^2}\right)}$$

If $y \to 0$, $\overline{OM} \to \overline{ME} \to \overline{PE} = \frac{R}{2}$ (P is the paraxial focus)

The longitudinal spherical aberration is

(5.29)
$$\overline{PM} = \frac{R}{2\left(1-\frac{y^2}{2R^2}\right)} - \frac{R}{2}$$

(5.30)
$$= \frac{y^2}{4R}$$

In the figure it was drawn the marginal ray to see it clearly, but it applies to any ray.

Calling η the transverse spherical aberration, is

(5.31)
$$\frac{\eta}{\overline{PM}} = \frac{2y}{R}$$

Then

(5.32)
$$\eta = \frac{y^3}{2R^2}$$

This is in the paraxial plane.

If the plane of intersection is displaced a quantity Δ, the new value of η is still given by the same proportionFig 5.12

(5.33)
$$\frac{\eta}{\overline{PM}-\Delta} = \frac{2y}{R}$$

Then

(5.34)
$$\eta = \frac{2y}{R}\left(\frac{y^2}{4R} - \Delta\right)$$

(5.35)
$$= \frac{y^3}{2R^2} - \frac{2y\Delta}{R}$$

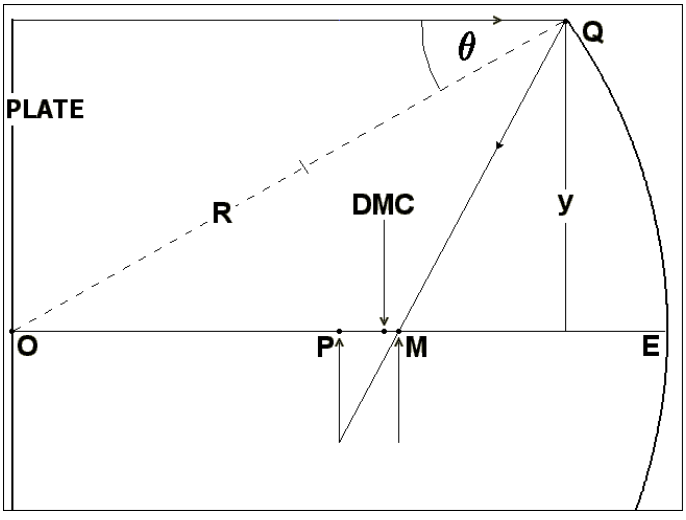

Fig. 5.12

It is wanted that all rays pass through the center of the disk of least confusion, for there the corrections to apply will be the least.

The value of Δ for this case is

(5.36)
$$\Delta = \frac{3}{4}\overline{PM}_{máx}$$

(5.37) $$= \frac{3\, y_m^2}{16\, R}$$

Where $y_m = y_{marginal}$. In that place is

(5.38) $$\eta = \frac{1}{2\, R^2}\left(y^3 - \frac{3\, y\, y_m^2}{4} \right)$$

The correction angle to the incident ray at height *y* is

(5.39) $$\alpha = \frac{2\,\eta}{R}$$

(5.40) $$= \frac{1}{R^3}\left(y^3 - \frac{3\, y\, y_m^2}{4} \right)$$

(There is a hidden approximation: $y_{plate} = y_{mirror} = y$)

This angle must be set by the plate, considered as a collection of prisms of index *n* and small angle ω . For this case is

(5.41) $$\alpha = (n-1)\,\omega$$

(5.42) $$= (n-1)\frac{dx}{dy}$$

Where *x* is the coordinate of the profile, or variation of plate thickness.

Then

(5.43) $$\frac{dx}{dy} = \frac{1}{(n-1)\,R^3}\left(y^3 - \frac{3\, y\, y_m^2}{4} \right)$$

That is

(5.44) $$x(y) = \frac{1}{4(n-1)R^3}\left(y^4 - \frac{3\, y^2 y_m^2}{2} \right)$$

This is the plate profile.

It is $\frac{dx}{dy} = 0$ for

(5.45) $$y = y_{neutral} = \frac{\sqrt{3}}{2}\, y_m = 0.866\, y_m$$

If $0 < y < y_{neutral}$ the plate is convergent and if $y_{neutral} < y < y_m$, is divergent.

The profile is then

(5.46) $$x(y) = A\, y^2 + B\, y^4$$

The central part is dominated by *A*, and it may be put

(5.47) $$A = \frac{1}{2\, R_c}$$

Where R_c is a very large central radius of curvature.

According to sign conventions, is $R_c > 0$ and $B < 0$ if the leading surface is carved.

With more technical terms, it may be put $R = 2f$, $y_m = D/2$, and results

(5.48) $$R_c = \frac{128\,(n-1)\,f^3}{3\, D^2}$$

(5.49) $$B = \frac{-1}{32\,(n-1)\,f^3}$$ (leading surface carved)

Exercise

To identify and discuss the approximations.

"Subtle is aberration theory, but not cheating", said a German.

Example

We shall study a Schmidt camera with the same focal distance as the refractor, but with a relative aperture *f / 3*. For this aperture or less the above formulae are valid. It will be used Schott UK 50 glass, with good transparency in the ultraviolet, and the working λ will be *3650; 4861; 5893 Å*. The refractive index of UK 50 in *4861 Å* is *n = 1.52859.* The camera is almost for photographic use; still there is no CCD as large to cover its field

Formulae (5.48) and (5.49) gives

$$R_c = 264226.8 \ mm$$

$$B = -3.15386 \times 10^{-11} \ mm^{-3}$$

The resulting prescription is

i	Radius curv.	Clear radius	Distance	Glass	Comment
1	*264226.8*	*200*	*23*	*UK50*	*ad*
2	*0*	*200*	*2466*	*1*	
3	*–2466*	*270*	*0*	*–1*	

Aspherics

i	Citric constant	Asf(4)	Asf(6)	Asf(8)
1	*–1*	-3.15386×10^{-11}	*0*	*0*

The mirror diameter permits a semi-field of 2.5 degrees without vignetting. The corresponding image is in Fig. 5.14 (b)

The plate has the profile shown in Fig. 5.13.

The maximum carved depth is *28.4 μm* .

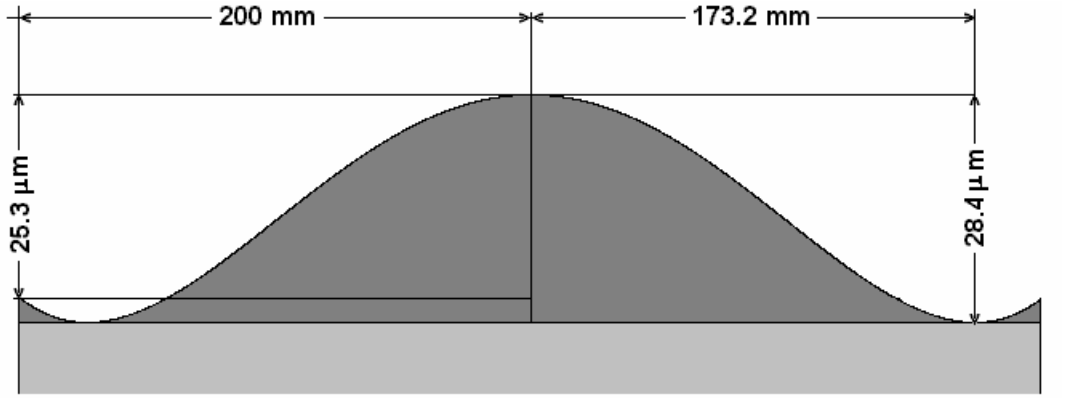

Fig. 5.13

Nevertheless, the effect of this small carving is amazing, as can be seen in Fig. 5.14 (a), where the plate has been withdrawn. The image is dominated by spherical aberration, and is nearly 40 times larger.

If the mirror is parabolized to cancel out this aberration, the resulting coma has the same extension as the corrected image for the tiny field of $0.031^{\circ} = 1.9'$.

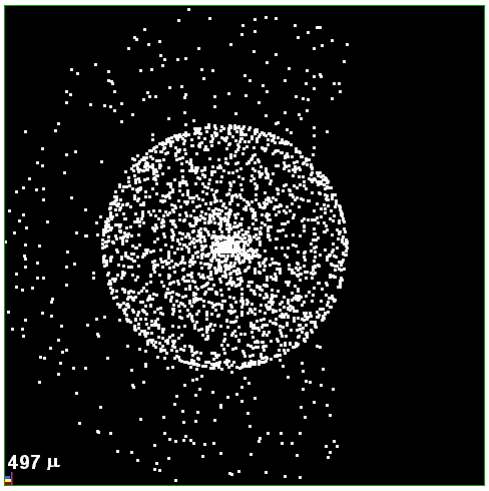

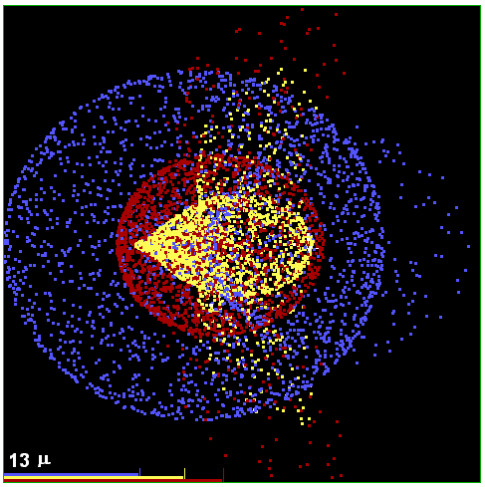

Fig. 5.14 (a) (b)

Compared with the apochromat, we see that the instrument is much more bulky, the image somewhat sharper, with luminosity 9 times larger over a field 25 times more extended.

If the relative aperture is larger than $\approx f/3$, the plate must have higher aspheric terms

Correctors with spherical meniscus

After the Schmidt invention, Bowers and Maksutov had the idea of using a thick meniscus with spherical surfaces instead of the aspheric plate. Such a lens has a small divergence, but an important spherical aberration opposite to that of the mirror. In particular, if the meniscus is concentric with the mirror, the dream of the system without axis is realized. In a system like this, all rays are meridional, and the image has only spherical and chromatic aberration, uniform over the whole field. Field curvature is no longer considered an aberration because it is part of the concentricity. The only design variables are the radii of curvature of the meniscus.

To obtain a concentric system replacing the Schmidt of the example, it must be found the pair of radius of curvature that minimizes the image, subject to the constraints imposed by the condition of concentricity. It is found that if

$$R_1 = -705\ mm$$

$$R_2 = -765\ mm,$$

The monochromatic images are as good as in the Schmidt, but the chromatic aberration is much worst.

The meniscus may be achromatized, as any lens, but then the concentricity is lost, what brings a degradation of the image towards the border of the field.

Hence one enters the specific process of optical design, that is, to change parameters and negotiate aberrations, taking into account the use to which the system is to be put, and the available resources.

The meniscus corrector requires a bulkier glass to grind, and this does not make it clearly preferable in spite of its theoretical simplicity.

For cameras of very large relative aperture, $f/1$ or more, there are often used compounded menisci and Schmidt plates. Menisci may be used in two symmetrical positions about the diaphragm.

There are also Cassegrain combinations of both types.

Field flattener lens

The large field systems as seen above are limited by chromatic aberration and field curvature. Field curvature in some astronomical cameras can be dealt with by deformation of the photographic plate by mechanical means, or also using a simple lens with its rear face flat in coincidence with the image.

It will be designed in a direct way, similar to what was done with the Schmidt plate.

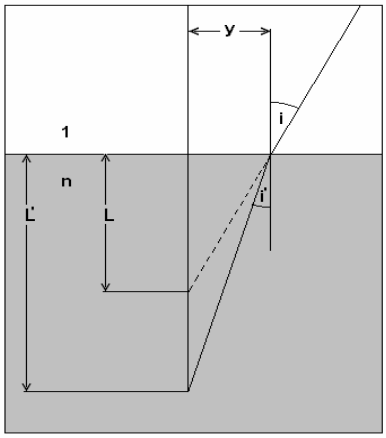

Fig. 5.15

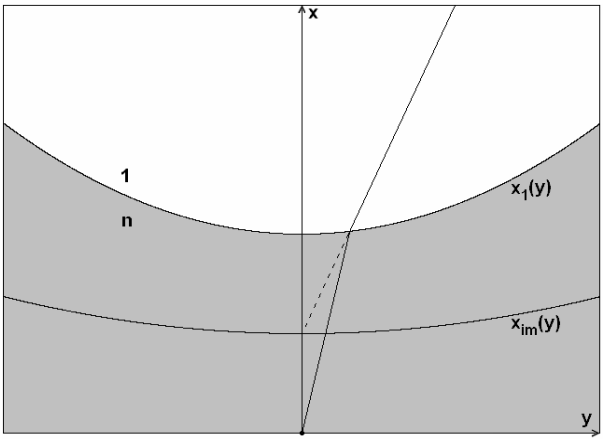

Fig. 5.16

With reference to Fig.(5.15) and (5.16), if angles *i, i'* are small, results

(5.50) $$i = \frac{y}{L} = n\, i' = \frac{n\, y}{L'}$$

(5.51) $$L' = n\, L :$$

Let $x_{im}(y)$ be the profile of the image surface, and $x_1(y)$ the profile of the anterior face of the lens.

(5.52) $$L' = x_1 = n\left(x_1 - x_{im}\right) = nL$$

(5.53) $$x_1 = \frac{n\, x_{im}}{n-1}$$

The flattened image surface coincides with the *y* axis.

In the extended paraxial region, x_1 and x_{im} are approximated by parabolas and $dx/dy \approx 0$.

Hence

(5.54) $$\frac{y^2}{2\,R_1} = \frac{n\, y^2}{2\,(n-1)\,R_{im}}$$

(5.55) $$R_1 = \frac{(n-1)\,R_{im}}{n}$$

R_1 is the radius of curvature of the anterior surface and R_{im} that of the image surface.

The axial thickness *d* is arbitrary but small, and the lens is placed so that *d* = *L'*

The sign of R_1 is that of R_{im} , and , for example, in the Schmidt camera the lens is plano-convex and in the Cassegrain telescope is plano-concave.

In practice it may be necessary for the rear face to be displaced from the image, for example to place a CCD detector or to avoid dirt or scratches to appear in the image.

The lens introduces lateral chromatism and coma, increasing with the displacement.

When a Schmidt camera is designed, the coma may be cancelled by displacing the plate, for in the original position it has no coma, and on approaching the mirror it has one of opposite sign to that of the lens. It results in a more compact system, a good notice.

Bibliography

"Principles of Optics" - M. Born y E. Wolf - Pergamon.
Modern Optical Engineering" - W. Smith - Academic Press.
Telescope Optics" - H. Rutten y M. van Venrooij – Willmann-Bell.
"Optical Astronomical Spectroscopy" - Kitchin - Institute of Physics Publishing - Bristol.
"Astronomical Optics" - Schroeder - Academic Press.
"Practical Computer Aided Lens Design" - G.H. Smith – Willmann-Bell.
"Achievements in Optics" – A. Bowers – Elsevier.
"Star Testing Astronomical Telescopes"- H. Suiter. – Willmann-Bell.
"Reflecting Telescope Optics". (2 Vol.) – R. N. Wilson -- Springer.